Journal of Materials Science & Technology xxx (2017) xxx–xxx

Contents lists available at ScienceDirect

Journal of Materials Science & Technology

journal homepage: www.jmst.org

Effect of grain size on mechanical property and corrosion resistance of the Ni-based alloy 690

Lv Jinlong

Fracture and Reliability Research Institute, School of Engineering, Tohoku University, Sendai 9808579, Japan

ARTICLE INFO

Article history:
Available online xxx

Keywords:
Alloys
Buffer
Deformation
Electrochemical impedance spectroscopy
Electrochemistry
Interfaces
Nanocrystalline
Oxidation

ABSTRACT

Mechanical property of coarse grained and nano/ultrafine grained alloy 690 and their corrosion resistance after immersion in high temperature borate buffer solution were investigated. The grain refinement significantly enhances the tensile strength of the alloy 690. In addition, the grain refinement facilitates the formation of the deformation twin which improves the ductility of the alloy 690. It has been found that the grain refinement promotes to form more Cr_2O_3 on the surface of the alloy 690 in high temperature borate buffer solution. At the same time, the grain refinement inhibits the formation of spinel type oxides. More hematite type oxides formed on nano/ultrafine grained alloy 690 improves its corrosion resistance in borate buffer solution. The hematite type oxides have a lower concentration of point defect than that of the spinel type oxides, which results in an excellent corrosion resistance of nano/ultrafine grained alloy 690. These results are supported by the Mott-Schottky analysis and the point defect model.

1. Introduction

The alloy 690 was first used as the substitute material for the alloy 600 in steam generator tubes [1]. Solid solution annealed alloy 690 exhibits excellent mechanical property [2]. The work hardening rate of the alloy 690 decreases with strain rate in the dynamic region with large strain level, which induces thermal softening [3], moreover, the dislocation and the twin densities increase as strain rate increases. The constitutive relation between the flow stress and the effective strain rate in the temperature range of 1273–1473 K was characterized for the alloy 690 [4]. Deformation of the coarse grained Ni based alloy is mainly achieved by the dislocation slip [5]. In addition, the mechanical twinning and interaction of the microtwins with the dislocations could be activated due to grain refinement [6,7]. Therefore, detailed deformation mechanism of grain refined alloy 690 is very complicated. The passive film formed on the alloy 690 affects its corrosion resistance [8] and stress corrosion cracking [9]. The study showed that ethanolamine (ETA) in NaOH solution promoted to form more oxides on the surface of the alloy 690, which improved its corrosion resistance [10]. The oxides on the alloy 690 showed a duplex layer structures with rich Ni and Fe in the outer layer and rich Cr in the inner layer after being exposed to aerated supercritical water [11]. The growth of outer layer oxides on the alloy 690 tubes in borated and lithiated high temperature water occurred by the precipitation mechanism [12]. The study revealed that the later-dissolved oxygen promoted the dissolution of protective Cr-rich oxides formed on the alloy 690 in the hydrogenated primary water if the corrosion potential increased [13]. The change of high temperature water also affects the structure of oxide formed on the alloy 690 [14]. The corrosion resistance of the alloy 690 in the simulated steam generators condition had been highly enhanced by the surface mechanical attrition treatment [15]. This was attributed to the fact that more grain boundaries provided a higher density of nucleation sites for the formation of a passive film and the diffusion paths for Cr. Our previous research showed that the grain refinement of the alloy 690 can promote the enrichment of Cr_2O_3 and inhibit the formation of $Cr(OH)_3$ in the passive films in borate buffer solution at room temperature, which improves the corrosion resistance of nano/ultrafine grained (NUG) alloy 690 [16].

Although nickel-based alloy 690 is widely used as a structural material for the steam generator tubes in nuclear power plant, the detailed deformation mechanism of grain refined alloy 690 has not clarified. Moreover, the pressurized water reactor primary water operates with H_3BO_3 as a chemical shim for excess thermal neutron absorption. Compared with the solution with chloride ion, the borate buffer solution is not easy to induce pitting corrosion. This facilitates to evaluate the passivation behavior of the Ni based alloy. The chemical composition and the microstructures of the oxides

E-mail address: ljltsinghua@126.com

https://doi.org/10.1016/j.jmst.2017.12.017
1005-0302/

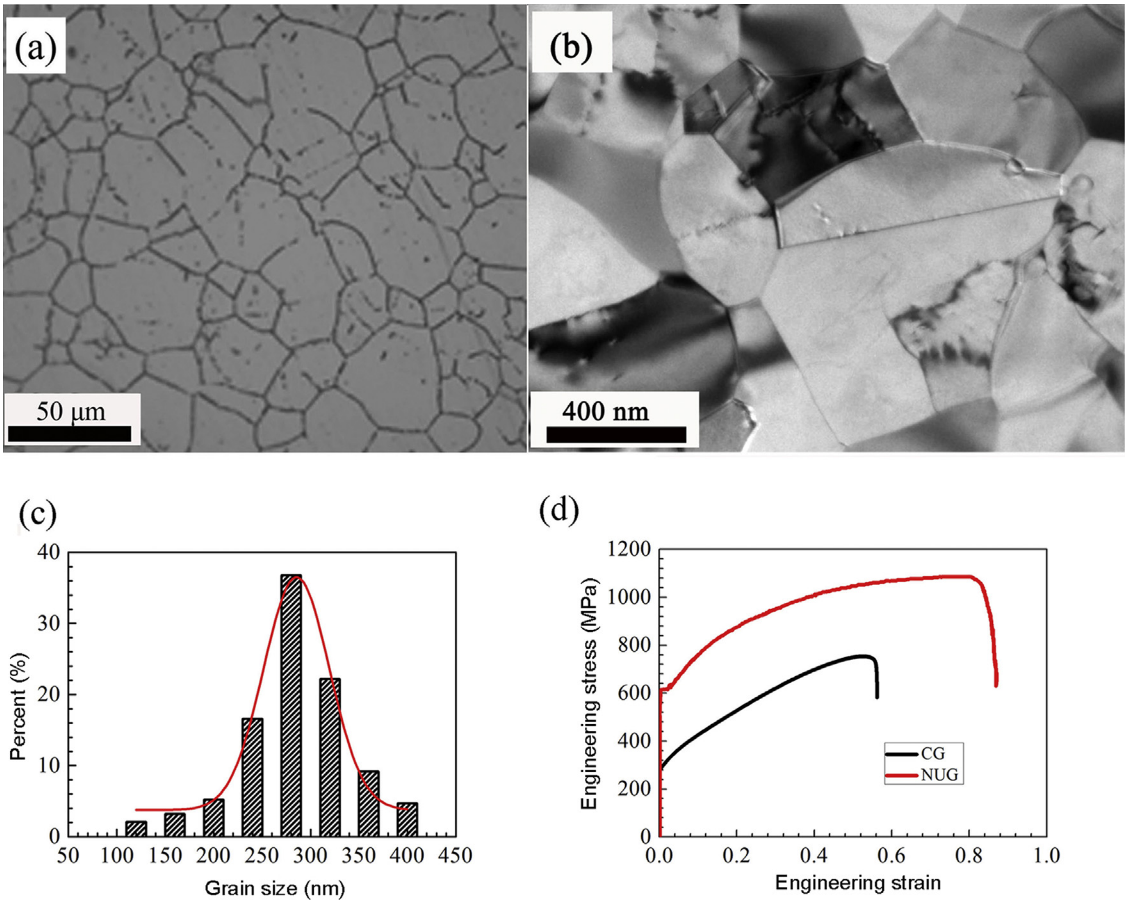

Fig. 1. (a) Microstructures of solid solution alloy 690, (b) TEM micrographs illustrating microstructure of NUG alloy 690, (c) grain size distribution of NUG alloy 690 and (d) engineering stress-strain curves of CG and NUG alloy 690.

significantly affect the corrosion resistance of the alloy 690. Therefore, the effect of the grain refinement on mechanical property of the alloy 690 and its corrosion resistance after being exposed to high temperature borate buffer solution will be evaluated in this study.

2. Experimental

The alloy 690 plate with a chemical composition (wt%): 0.03C, 0.28 Si, 0.25 Mn, 29.0 Cr, 0.02 Cu, 9.5 Fe, 0.002 S and balance Ni was used for test. The coarse grained (CG) samples were obtained by solution annealing at 1100 °C for 1 h in vacuum and subsequently quenching into water. The nano/ultrafine grained (NUG) alloy 690 was obtained by 90% total thickness reduction of CG sample in a laboratory rolling mill and annealing at 800 °C for 500 s. Dog-bone-shaped samples with a gauge section of 80 mm in length and 20 mm in width were subjected to a continually increasing tensile strain in a Instron 8862 system of 50 kn capacity at a strain rate of 1×10^{-4} s^{-1}. The elongation of the gauge length was measured by a contact clip-on extensometer at room temperature. Microhardness tests were carried out using a load of 100 gf and the dwell time for 10 s. The average hardness value was reported by five measurements. A JEM-2100F transmission electron microscopy (TEM) was used to examine the microstructures. Coupon type samples (10 mm × 10 mm) were exposed to high temperature borate buffer solution in autoclaves. The used electrolyte solution was pH 8.4 borate buffer solution (0.075 mol L^{-1} $Na_2B_4O_7$ + 0.3 mol L^{-1} H_3BO_3). In order to decrease the effect of dissolved oxygen (DO), the autoclave was deoxygenized by purging with N_2 gas for 2 h before the test. DO in the inlet water was controlled at <5 ppb. Then test was performed at 300 °C and 12 ± 0.5 MPa for 20 days. The coarse grained oxidized (CG—O) and nano/ultrafine grained oxidized (NUG-O) represent the oxidized samples. The surface morphology of the oxides formed on the alloy 690 was examined by a field emission scanning electron microscopy (FE-SEM) of LEO-1530. The analysis of the corrosion products was performed in a Rigaku Ultima IV X-Ray diffraction (XRD) system using K_α (0.154056 nm) radiation at 40 kV and 40 mA. A Raman spectroscopy (Renishaw InVia Raman Microscope System) with 633-nm excitation wavelength was also used to characterize oxides.

A saturated calomel electrode (SCE) was used as the reference electrode. A thin platinum foil served as the counter electrode. The electrolyte in the investigation was also pH 8.4 borate buffer solution. A CHI 660E electrochemical station (Chenhua instrument Co. Shanghai, China) was used. The electrochemical impedance spectroscopy (EIS) experiments were conducted over the frequency from 100 kHz to 10 mHz with a 5 mV (peak to peak) amplitude signal. A Zsimpwin software was used to fit obtained EIS data.

3. Results and discussion

Fig. 1(a) shows a typical microstructure of solid solution alloy 690, and the average grain size of solid solution one is 30 μm. Fully recrystallized alloy 690 with refined grain size is shown in Fig. 1(b). The statistical distribution of nano/ultrafine grain for the alloy 690 is shown in Fig. 1(c). The grain size distribution shows an obvious peak, and the average grain size is 280 nm. The engineering stress–strain plots for CG and NUG alloy 690 are presented in